

RESEARCH

Open Access



Identification and validation of hub m7G-related genes and infiltrating immune cells in osteoarthritis based on integrated computational and bioinformatics analysis

Zhenhui Huo^{1†}, Chongyi Fan^{2†}, Kehan Li¹, Chenyue Xu¹, Yingzhen Niu^{1*} and Fei Wang^{1*}

Abstract

Background Osteoarthritis (OA) is a joint disease closely associated with synovial tissue inflammation, with the severity of synovitis impacting disease progression. m7G RNA methylation is critical in RNA processing, metabolism, and function, but its role in OA synovial tissue is not well understood. This study explores the relationship between m7G methylation and immune infiltration in OA.

Methods Data were obtained from the GEO database. Hub genes related to m7G were identified using differential expression and LASSO-Cox regression analysis, and a diagnostic model was developed. Functional enrichment, drug target prediction, and target gene-related miRNA prediction were performed for these genes. Immune cell infiltration was analyzed using the CIBERSORT algorithm, and unsupervised clustering analysis was conducted to examine immune infiltration patterns. RT-qPCR was used to validate hub gene expression.

Results Seven m7G hub genes (SNUPN, RNMT, NUDT1, LSM1, LARP1, CYFIP2, and CYFIP1) were identified and used to develop a nomogram for OA risk prediction. Functional enrichment indicated involvement in mRNA metabolism and RNA transport. Differences in macrophage and T-cell infiltration were observed between OA and normal groups. Two distinct m7G immune infiltration patterns were identified, with significant microenvironment differences between clusters. RT-qPCR confirmed differential hub gene expression.

Conclusion A diagnostic model based on seven m7G hub genes was developed, highlighting these genes as potential biomarkers and significant players in OA pathogenesis.

Keywords Osteoarthritis, Bioinformatics, M7G, Immune cell infiltration, Differentially expressed genes

[†]Zhenhui Huo and Chongyi Fan contributed equally to this work.

*Correspondence:

Yingzhen Niu

niuyingzhen@yeah.net

Fei Wang

wangfei@hebmh.edu.cn

¹ Department of Orthopaedic Surgery, Third Hospital of Hebei Medical University, Shijiazhuang, Hebei 050051, China

² Department of Orthopedics, Aerospace Central Hospital, Beijing 100049, China



Introduction

Osteoarthritis (OA) is the most prevalent form of arthritis and a leading degenerative joint disease, often characterized by pain, joint deformity, and disability [1]. While traditionally viewed as a cartilage-centric disorder [2], growing evidence indicates that OA is a whole-joint disease, affecting not only articular cartilage but also subchondral bone, synovium, meniscus, and the infrapatellar fat pad (IPFP) in a complex pathological process [3]. Synovial tissue plays a central role in OA, as interactions within the synovial membrane trigger the release of soluble mediators, driving inflammation [4]. The severity of synovitis is a key indicator of disease progression, emphasizing its crucial role in OA pathogenesis. Among the joint structures implicated in OA, the IPFP has gained recognition as more than just a mechanical shock absorber; it functions as an immunoreactive organ, closely interacting with the synovial membrane to form an anatomic-functional unit that modulates inflammation.

OA develops and progresses due to multiple risk factors, including aging, obesity, genetic predisposition, joint injuries, and metabolic disturbances [5, 6]. Among these, aging is a major contributor, as aged chondrocytes exhibit reduced regenerative capacity and increased susceptibility to oxidative stress [7]. Obesity accelerates OA not only through excessive mechanical loading but also via metabolic inflammation driven by adipokines [8]. Genetic predisposition influences OA by identifying key risk loci involved in cartilage homeostasis and inflammatory signaling [9]. Joint injuries, such as meniscal tears or anterior cruciate ligament ruptures, exacerbate OA by triggering inflammatory cascades and joint instability [10]. Additionally, metabolic conditions like diabetes and dyslipidemia promote OA through systemic inflammation and oxidative stress [11].

The immune system plays a pivotal role in OA progression, with chronic inflammation acting as a key driver of symptom exacerbation and disease advancement [12]. In OA, the synovial membrane exhibits persistent inflammation, attracting immune cells such as macrophages, neutrophils, and lymphocytes. These infiltrating cells release pro-inflammatory cytokines (e.g., IL-1 β , TNF- α , IL-6) and chemokines, further disrupting immunological homeostasis and accelerating cartilage degradation, subchondral bone remodeling, and osteophyte formation [13]. This inflammatory environment extends beyond the synovium, affecting the cartilage, infrapatellar fat pad, and meniscus, reinforcing the view that OA is a systemic joint disease, rather than a localized cartilage disorder [14, 15].

RNA modification is a common post-transcriptional process in eukaryotes that has garnered increasing research interest. Among these modifications, RNA

methylation plays a pivotal role in disease progression, significantly impacting RNA splicing, subcellular distribution, degradation, stability, and translation [16, 17]. Emerging evidence suggests a link between RNA modifications and inflammatory diseases, including OA [18], highlighting the need to investigate epigenetic factors influencing OA progression and treatment response. Among RNA methylation types, m6A and m7G are the most prevalent [19, 20]. Research on m6A has been more extensive, whereas investigations into m7G remain relatively limited. The m7G nucleotide is primarily found in tRNAs and rRNAs, where it plays a pivotal role in regulating various aspects of mRNA metabolism throughout its life cycle. Notably, m7G cap modifications are frequently observed in mRNAs associated with OA [21], exerting significant influence over translation efficiency, splicing, and mRNA stability [20]. Furthermore, m7G modifications modulate the synthesis of OA-related proteins by regulating RNA-binding proteins [22, 23], thereby affecting the translation of inflammatory mediators and cartilage matrix components. Emerging evidence underscores the critical involvement of m7G modifications in a wide range of biological processes, including immune cell infiltration, immunotherapeutic responses, inflammatory regulation, and antitumor activity [20, 24]. These functional effects are largely mediated through intricate interactions among m7G RNA methylation regulators. Consequently, elucidating the precise mechanisms underlying m7G modifications in OA is essential for advancing our understanding of disease pathogenesis and progression.

With the advancement of microarray sequencing and bioinformatics, numerous studies have leveraged these technologies to identify novel biomarkers, uncover epigenetic alterations, and elucidate molecular mechanisms in various diseases. Recent findings highlight the potential of dysregulated genes and proteins in OA as diagnostic markers and therapeutic targets.

In this study, we identified seven m7G hub genes (SNUPN, RNMT, NUDT1, LSM1, LARP1, CYFIP2, and CYFIP1) in OA through differential expression analysis and LASSO Cox regression. We evaluated their predictive potential and developed a diagnostic model. Further analyses, including functional enrichment, immune infiltration, drug target prediction, and miRNA prediction, were conducted to explore their roles in OA pathogenesis. Additionally, we classified OA patients into two m7G modification subtypes and performed immune infiltration and gene set enrichment analysis (GSEA) to characterize their molecular profiles. Finally, we validated the expression of these seven hub genes using real-time quantitative polymerase chain reaction (RT-qPCR).

Materials and methods

Data acquisition

The Gene Expression Omnibus (GEO) (<http://www.ncbi.nlm.nih.gov/geo/>) is a public genomics database that stores gene expression profiles, raw sequences, and platform information. Using the keyword “OA” in the GEO database, datasets containing synovial tissue samples from both normal individuals and OA patients were retrieved, based on the following criteria: (1) Homo sapiens; (2) RNA expression profiling by microarray; (3) OA or normal tissue samples. A total of eight OA-related datasets were downloaded for this study (Table 1). Six datasets were used as training cohorts, while two datasets were used as independent validation cohorts. All eight datasets consisted of human knee synovial tissue samples.

Data integration and pre-processing

In this study, each of the six datasets was annotated using Perl software to map probes to the platform annotation information, converting probe names into gene names. The datasets were then merged using the “inSilicoMerging” package in R, and batch effects were corrected using the Johnson WE method to eliminate systematic differences between studies [25]. The resulting batch-corrected matrix was then processed using the robust multi-array averaging algorithm in the “limma” package to generate expression data for further analysis. For genes with multiple corresponding probes, the average expression value was used. The final integrated dataset consisted of 39 normal samples and 41 OA samples.

Differential expression analysis

A total of 40 m7G-related genes (Additional file 1: Table S1) were compiled from the gene sets GOMF_RNA_CAP_BINDING, GOMF_RNA_7_METHYLGUANOSINE_CAP_BINDING, GOMF_M7G_5_PPPN_DIPHOSPHATASE_ACTIVITY, and

GOBP_7_METHYLGUANOSINE_RNA_CAPPING. Given that our study focuses on knee synovial tissue samples in OA, we screened these 40 genes across six OA-related datasets to ensure relevance and reliability. Genes with available expression data in at least one dataset were retained, while those with undetectable expression (i.e., missing or below detection limits across all datasets) were excluded. We investigated the association between m7G RNA methylation regulators and disease progression, as well as their co-expression patterns. A protein–protein interaction (PPI) network was constructed using the STRING database [26] to explore interactions among these regulators, which are involved in biological signaling, gene expression control, metabolism, and cell cycle regulation. The PPI network was then visualized using Cytoscape (v3.0.0) [27]. To identify OA-related and significant m7G differentially expressed genes (DEGs), we conducted differential expression analysis using the “limma,” “reshape2,” and “ggpubr” packages in R. The resulting expression data were formatted into ggplot2 input files to generate heat maps and box plots for visualization. Additionally, the “circus” package in R was used to map the chromosomal localization of m7G DEGs [28].

Identification of m7G hub genes for the diagnosis of OA

Based on the expression levels of DEGs, univariate logistic regression was performed using the “rms” R package to identify m7G hub genes closely associated with OA occurrence. To further refine gene selection and prevent overfitting, we applied LASSO Cox regression analysis using the “glmnet” R package, which employs L1 regularization to penalize the number of variables included in the model. To determine the optimal lambda (λ) value, tenfold cross-validation was conducted, selecting lambda_min, which corresponds to the smallest mean cross-validated error. This method ensures that only the most predictive genes with nonzero coefficients are retained. The risk score performance in differentiating OA patients from healthy individuals was assessed using Receiver Operating Characteristic (ROC) curve analysis with the “pROC” package in R. A high predictive ability was indicated by an area under the curve (AUC) > 0.7 and $P < 0.05$. The diagnostic efficacy of the model was further validated using two independent validation cohorts through ROC curve analysis.

Construction of the nomogram model

The nomogram prediction model, based on multivariate analysis, integrates multiple predictors to estimate the probability of disease occurrence in individual patients [29]. A risk prediction model was developed using the seven key m7G-related genes, with the “rms” package employed to construct a nomogram for predicting OA

Table 1 Characteristics of GEO datasets included in the study

Type	Series	Platform	NOR	OA	Species
Training cohort	GSE1919	GPL91	5	5	Homo sapien
Training cohort	GSE55235	GPL96	10	10	Homo sapien
Training cohort	GSE82107	GPL570	7	10	Homo sapien
Training cohort	GSE55457	GPL96	10	10	Homo sapien
Training cohort	GSE77298	GPL570	7	0	Homo sapien
Training cohort	GSE55584	GPL96	0	6	Homo sapien
Total			39	41	
Validation cohort	GSE12021	GPL96	9	10	Homo sapien
Validation cohort	GSE12021	GPL97	4	10	Homo sapien

incidence. To assess the model's accuracy and reliability, a calibration curve was generated to compare predicted and actual values, ensuring consistency. Each characteristic gene was assigned a score within the nomogram model, where higher scores corresponded to a higher likelihood of OA, allowing for an evaluation of the model's clinical utility in guiding patient-specific decision-making.

Function enrichment analysis

Gene ontology (GO) was employed to analyze the hub genes from three aspects: biological process (BP), cellular component (CC), and molecular function (MF) [30]. Kyoto encyclopaedia of genes and genomes (KEGG) [31] was applied to explore the hub genes-related pathways and high level biological functions. The background gene sets selected the GO annotations from SangerBox (version 3.0) platform (<http://vip.sangerbox.com/home.html>) and the latest KEGG pathway gene annotations that were obtained from KEGG rest API (<https://www.kegg.jp/kegg/rest/keggapi.html>). Enrichment analysis was fulfilled with SangerBox platform [32]. The maximum and minimum gene set sizes were set to 5,000 and 5, respectively, and the threshold of statistical significance was set to P Value < 0.05 and FDR < 0.05.

Prediction of drug and miRNAs targets

Drug target prediction of hub genes was performed through the Enrichr website (<https://maayanlab.cloud/Enrichr/>). We used miRNet (<https://www.mirnet.ca/>) [33], a tool that integrates data from 11 different miRNA databases, to predict regulatory miRNAs of the common hub-genes.

Immune cell infiltration analysis

The immune microenvironment comprises immune cells, inflammatory cells, fibroblasts, mesenchymal cells, cytokines, and chemokines, playing a crucial role in disease progression and treatment response. Immune cell infiltration analysis is particularly valuable for understanding OA pathology and therapeutic targets. To estimate the proportion of immune cells in OA samples, we applied the CIBERSORT algorithm, which utilizes linear support vector regression to deconvolute gene expression profiles from RNA-sequencing data [34]. The relative abundance of 22 immune cell types was calculated and visualized using histograms and box plots, comparing OA and normal groups. Finally, we used the "corrplot" package in R to perform a Spearman correlation analysis, examining relationships between infiltrating immune cells and m7G RNA methylation regulators.

Identification of m7G modification patterns in OA

Based on the expression profiles of seven m7G hub genes, unsupervised consensus clustering analysis was conducted to identify distinct m7G modification patterns in OA samples. Clustering was performed using the "ConsensusClusterPlus" package, with 1,000 iterations on 80% of the samples to ensure stability and robustness [35]. To further characterize these modification patterns, Principal Component Analysis (PCA) was applied to assess the expression profiles of 22 m7G RNA methylation regulators, leading to the classification of the OA cohort into two distinct patterns. A PCA-based scoring system was then developed to quantify m7G modification patterns in individual patients. Box plots were used to visualize differences in m7G RNA methylation regulator expression across patterns. Finally, the levels of 22 immune cell types were compared between the two m7G modification patterns to explore their association with immune infiltration in OA.

Pathway enrichment analysis in m7G modification patterns

GSEA was performed using GSEA v3.0 (<http://www.broadinstitute.org/gsea>) [36] and downloaded the c2.cp.kegg.v7.4.symbols.gmt and c2.cp.reactome.v7.4.symbols.gmt subsets from the Molecular Signatures Database (<http://www.gsea-msigdb.org/gsea/downloads.jsp>) [37] to evaluate the related pathways and molecular mechanisms of different clusters. The statistical significance was assessed using a significance level of $P < 0.05$.

Sample collection

Synovial tissues from 3 patients with meniscus injury and 3 patients undergoing total knee arthroplasty due to OA were collected from the Third Hospital of Hebei Medical University. All patients were strictly read and signed informed consent and approved by the Ethics Committee of the Third Hospital of Hebei Medical University. The research followed the guidelines of the 1975 Declaration of Helsinki.

RNA extraction and gene expression analysis

The synovial tissue samples were subjected to RNA isolation using Redzol Reagent (SBS, Beijing, China) to obtain total RNA. The quality and concentration of the extracted RNA were assessed using a NanoDrop spectrophotometer. Complementary DNA was synthesized using the SureScript RTase Mix and SureScript RT Reaction Buffer following the manufacturer's protocol. The primer sequences for the genes can be found in Additional file 1: Table S2. RT-qPCR was performed using the 2 × SYBR Green qPCR Master Mix (None ROX) (Servicebio, Wuhan, China), with GAPDH

-serving as the endogenous reference gene for normalization. The $2^{-\Delta\Delta CT}$ method was used to calculate relative gene expression levels. All experiments were performed in triplicate, and data were presented as mean \pm standard deviation. Statistical analysis was conducted using GraphPad Prism 9.0, with an independent Student's t-test applied to compare gene expression levels between OA and normal samples. $P < 0.05$ were considered statistically significant.

Statistical analysis

All statistical analyses in our study were performed with R software (version 4.3.1). To compare two groups of continuous variables, statistical significance of normally distributed variables was calculated using an independent Student's t-test, and differences between non-normally distributed variables were calculated using the Wilcoxon rank-sum test. The chi-square test or Fisher's exact test was carried out to analyze the statistical significance between two sets of categorical variables. Correlation coefficients between different genes were estimated via Spearman correlation analysis. All statistical P values were two-sided, and $P < 0.05$ was considered statistically significant. For all figures: * represents $P < 0.05$, ** represents $P < 0.01$, *** represents $P < 0.001$, and **** represents $P < 0.0001$.

Results

Differential analysis of m7G RNA methylation regulators

Batch effects were removed from the GEO dataset to obtain an integrated dataset comprising 41 OA samples and 39 normal samples (Fig. 1). Prior to batch effect correction, Uniform Manifold Approximation and Projection (UMAP) analysis showed that samples clustered by dataset, indicating the presence of significant batch effects (Fig. 1A, C). After batch correction, the distribution of samples became more intermixed across datasets, demonstrating that batch effects were effectively mitigated while preserving biological variation (Fig. 1B, D). The improved clustering of OA and normal samples, independent of dataset origin, further supports the effectiveness of this batch effect removal process. A total of 22 m7G RNA methylation regulators with statistically available expression data were identified across datasets: WDR4, SNUPN, RNMT, RNGTT, NUDT4, NUDT3, NUDT1, NCBP2, NCBP1, METTL1, LSM1, LARP1, IFIT5, EIF4G3, EIF4E2, EIF4E, EIF3D, DCP2, CYFIP2, CYFIP1, CMTR1, and AGO2. These genes were subsequently analyzed for differential expression, correlation patterns, and functional enrichment. The PPI network, constructed from these 22 m7G RNA methylation regulators, consisted of 22 nodes and 108 edges (Fig. 2A), with NCBP2, NCBP1, EIF4E2, EIF4E, and DCP2 identified as the most highly connected nodes. Through differential

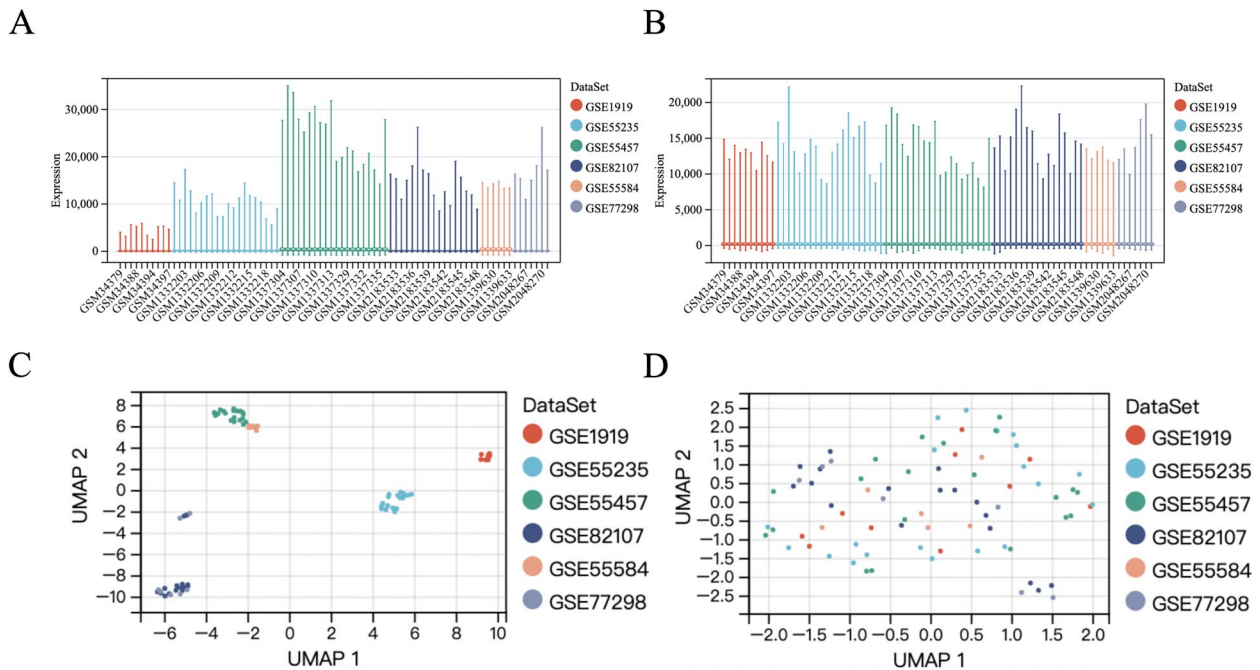


Fig. 1 GEO data de-batching. **A** Gene expression level statistics of the dataset before de-batching. **B** Gene expression level statistics of the integrated dataset after de-batching. **C** Uniform Manifold Approximation and Projection (UMAP) between datasets before de-batching. **D** UMAP between integrated datasets after de-batching

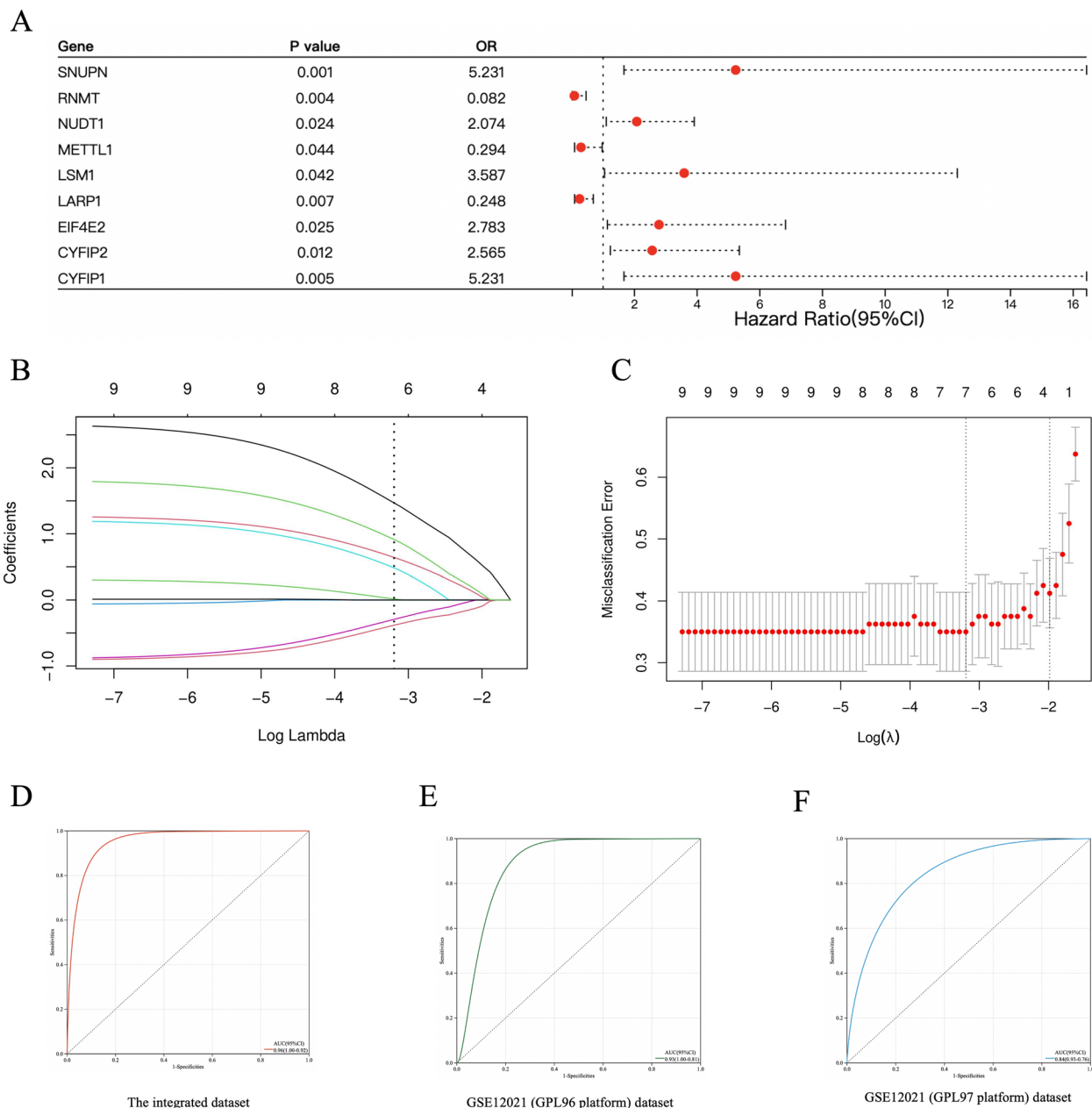


Fig. 3 Construction and validation of diagnostic models. **A** The logistic regression analysis of the nine m7G hub genes. **B, C** Screening of hub genes from DEGs using the LASSO Cox regression analysis. **D** ROC curve of the diagnostic model in the training cohort in OA diagnosis. **E, F** ROC curves of the diagnostic model in external validation cohorts in OA diagnosis

process, regulation of neurotrophin TRK receptor signaling pathway, neurotrophin TRK receptor signaling pathway, dendrite extension, neurotrophin signaling pathway, vascular endothelial growth factor receptor signaling pathway and dGTP catabolic process (Fig. 5A). For the CC of GO terms, these genes were mostly related to mRNA and RNA cap binding

complex (Fig. 5B). With regards to the ME, the genes were mostly related to RNA binding, RNA cap binding and translation regulator activity (Fig. 5C). The KEGG results showed that the genes were mainly related to RNA transport, Pathogenic Escherichia coli infection, Regulation of actin cytoskeleton, RNA degradation and mRNA surveillance pathway (Fig. 5D).

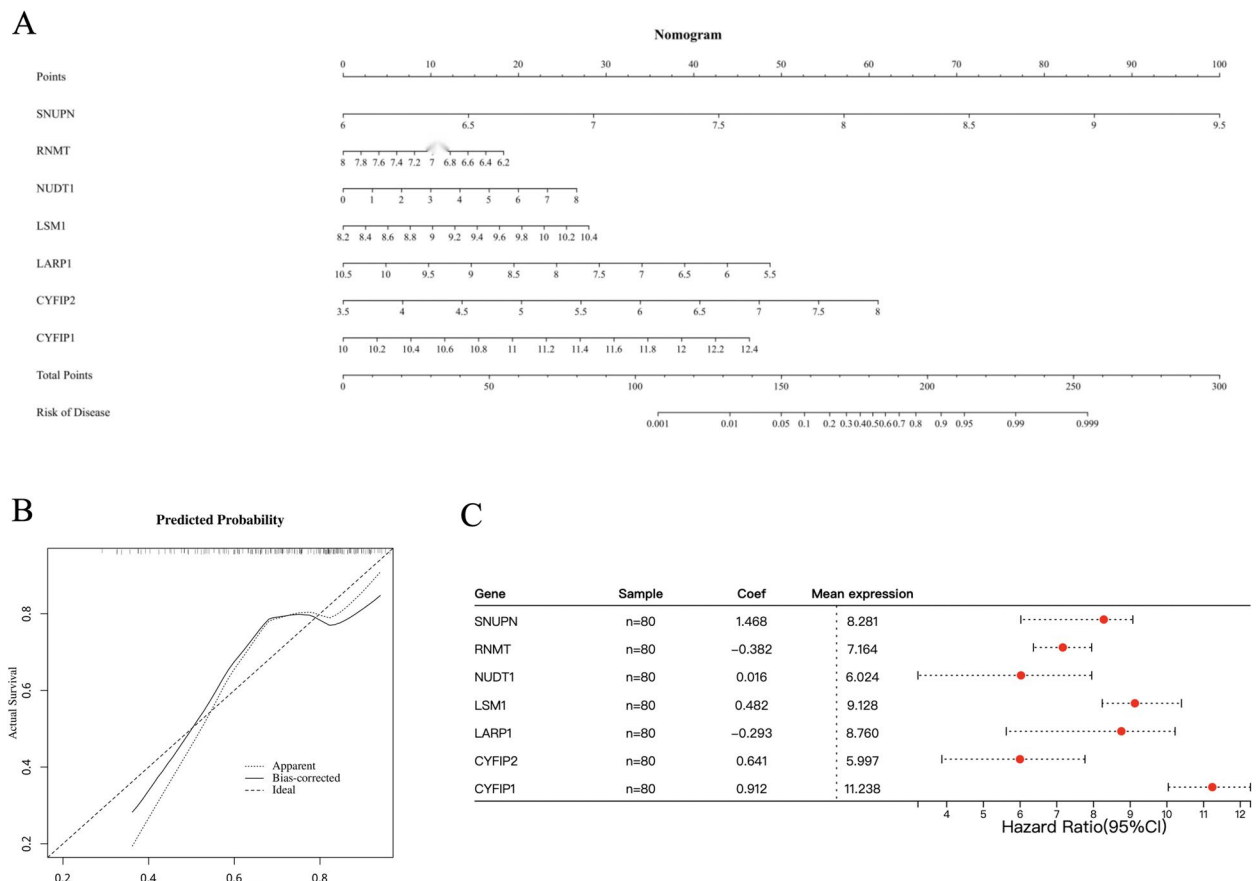


Fig. 4 Construction of the nomogram model. **A** A nomogram model constructed based on the seven hub genes. **B** Calibration curve of the column line graph. **C** Forest plot of seven hub genes in OA patients

Prediction of characteristic genes related targets

For drug target prediction, chlortetracycline HL60 DOWN, PARAQUAT CTD 00006471, baclofen HL60 DOWN and other candidate molecules were predicted to have potential therapeutic effects because they had the highest odds ratio and the highest comprehensive score (Table 2). We applied the miRNet database to screen the targeted miRNAs of SNUPN, RNMT, NUDT1, LSM1, LARP1, CYFIP2 and CYFIP1. A total of 286 miRNAs were predicted, 24 miRNAs with association with three or more genes. Finally, the network of characteristic genes and potential miRNAs-targeted was visualized (Fig. 6).

Differences in immune characteristics

The CIBERSORT analysis revealed that the levels of resting CD4+memory T cells, activated mast cells, and eosinophils were significantly lower in the OA group compared to the normal group (Fig. 7A, B). Conversely, the levels of activated CD4+memory T cells, regulatory T cells (Tregs), M0 macrophages, M1 macrophages, and resting mast cells were significantly higher in the OA

group (Fig. 7A, B). Furthermore, we calculated the correlation between immune cell contents (Fig. 7C). There was a significant positive correlation between activated CD4+memory T cells and naive CD4+T cells ($r=0.79$) and a significant negative correlation between resting mast cells and activated mast cells ($r=-0.69$). Additionally, the analysis of the seven m7G hub genes revealed that they were closely related to several immune cells in the OA group (Fig. 7D). CYFIP2 showed the strongest positive correlation with memory B cells ($r=0.50$), while NUDT1 had the strongest negative correlation with naive B cells ($r=-0.43$).

Identification of m7G modification patterns

To further validate m7G methylation modification patterns in OA patients, we used consensus clustering on seven m7G hub regulators, dividing OA patients into two distinct patterns (C1 and C2) based on optimal clustering stability ($k=2$; Fig. 8A-C). Among 41 OA patients, 29 were classified as C1 and 12 as C2. A heat map illustrated the expression levels of m7G hub genes in these two patterns (Fig. 8D), while PCA confirmed

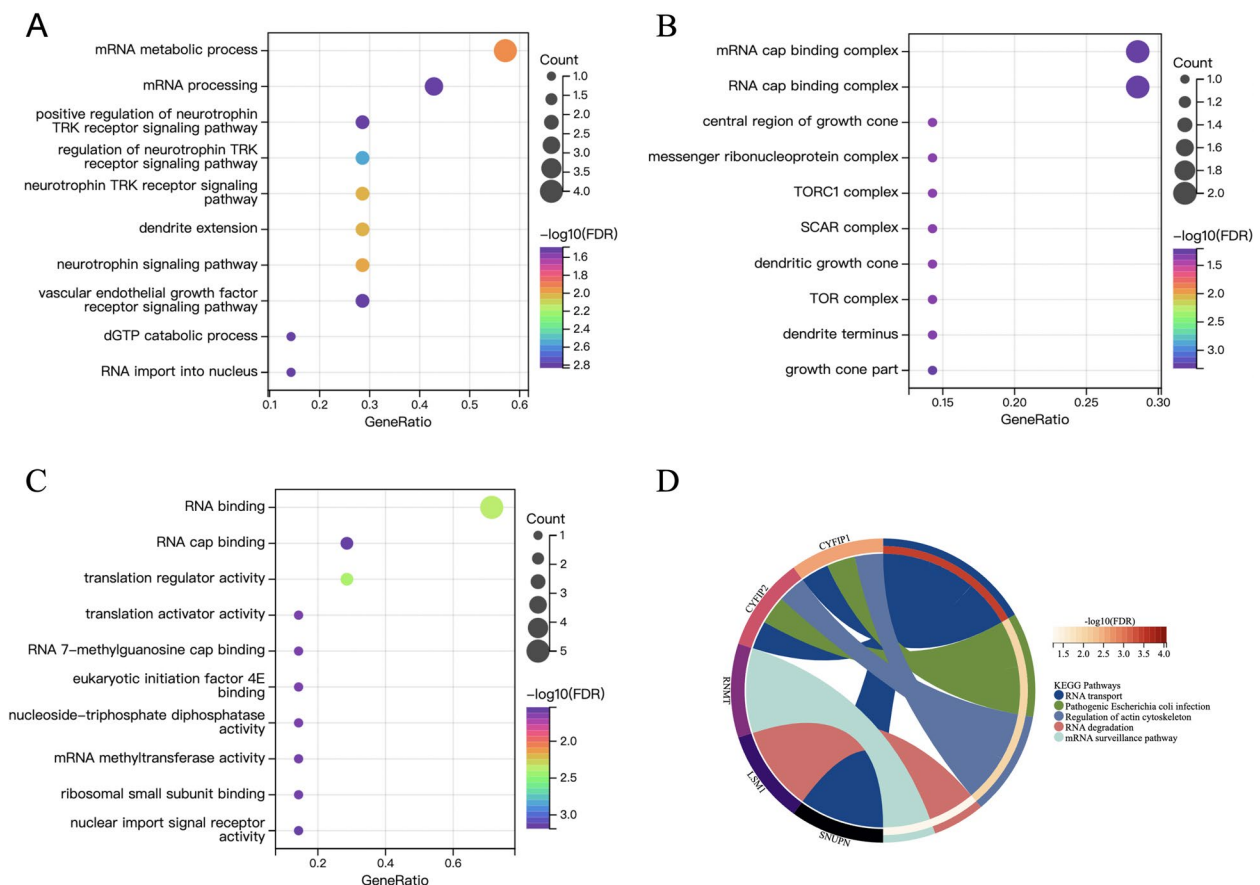


Fig. 5 GO and KEGG pathway enrichment analysis of seven hub genes. **A-C** GO analysis of the following components: BP, biological process (**A**); CC, cellular component (**B**); and MF, molecular function (**C**). **D** KEGG analysis

Table 2 The drug signatures database analysis of seven m7G hub genes

Description	P value	Odds Ratio	Combined Score
Chlortetracycline HL60 DOWN	2.33E-04	24.151689	202.050365
Paraquat CTD 00006471	2.29E-03	37.5014218	228.000274
Baclofen HL60 DOWN	2.75E-03	34.0706897	200.840176
5-Amino-2-methylphenol CTD 00004911	3.84E-03	333.05	1852.15668
Rescinnamin CTD 00003038	4.54E-03	277.513889	1497.0326
Rescinnamin TTD 00010545	4.89E-03	256.153846	1362.86237
Cloпамide HL60 DOWN	5.88E-03	22.9154519	117.683872
Pinaflavol TTD 00010236	6.63E-03	184.953704	927.700129
LY-294002 HL60 UP	7.68E-03	158.507937	771.885508
Reserpine TTD 00010547	8.02E-03	151.295455	730.060221

clear separation between C1 and C2 (Fig. 8E). Significant differences in the expression of the seven hub genes between C1 and C2 verified the clustering accuracy (Fig. 8F). Specifically, RNMT, LARP1, LSM1, CYFIP2, and CYFIP1 showed higher expression in

C1, whereas SNUPN and NUDT1 were more highly expressed in C2, indicating that C1 had overall upregulated m7G hub genes. Furthermore, we found that the m7G score was associated with these modification patterns, with C1 showing a higher m7G score than C2 (Fig. 9B).

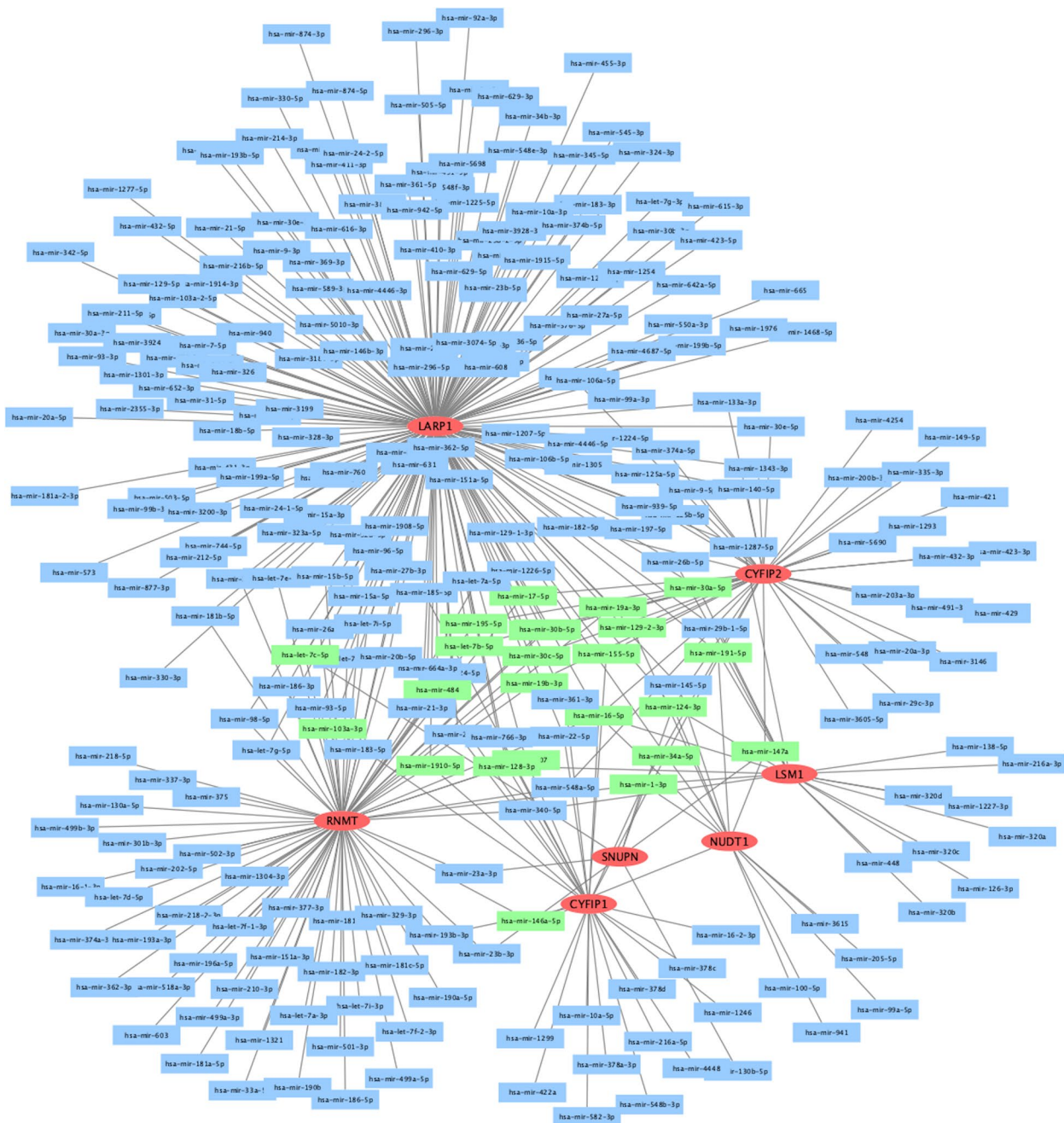


Fig. 6 Screening of potential miRNAs targeting seven m7G hub genes. An interaction network of hub genes and potential miRNAs-targeted. Red represented m7G hub genes, blue represented all miRNAs, and green represented miRNAs associated with three or more genes

Identification of the immune characteristics of two modification patterns

The CIBERSORT algorithm was used to analyze immune cell infiltration in the two distinct m7G modification patterns, revealing significant differences in immune composition between the groups. C1 patients exhibited lower levels of activated natural killer (NK) cells compared to

C2, while resting mast cells and naive B cells were significantly more abundant in C1 (Fig. 9A). Further correlation analysis of immune cell populations showed that in C1 patients, monocytes and eosinophils had a strong positive correlation ($r=0.79$), whereas activated NK cells and M0 macrophages were negatively correlated ($r=-0.64$) (Fig. 9C). In contrast, in C2 patients, gamma delta T

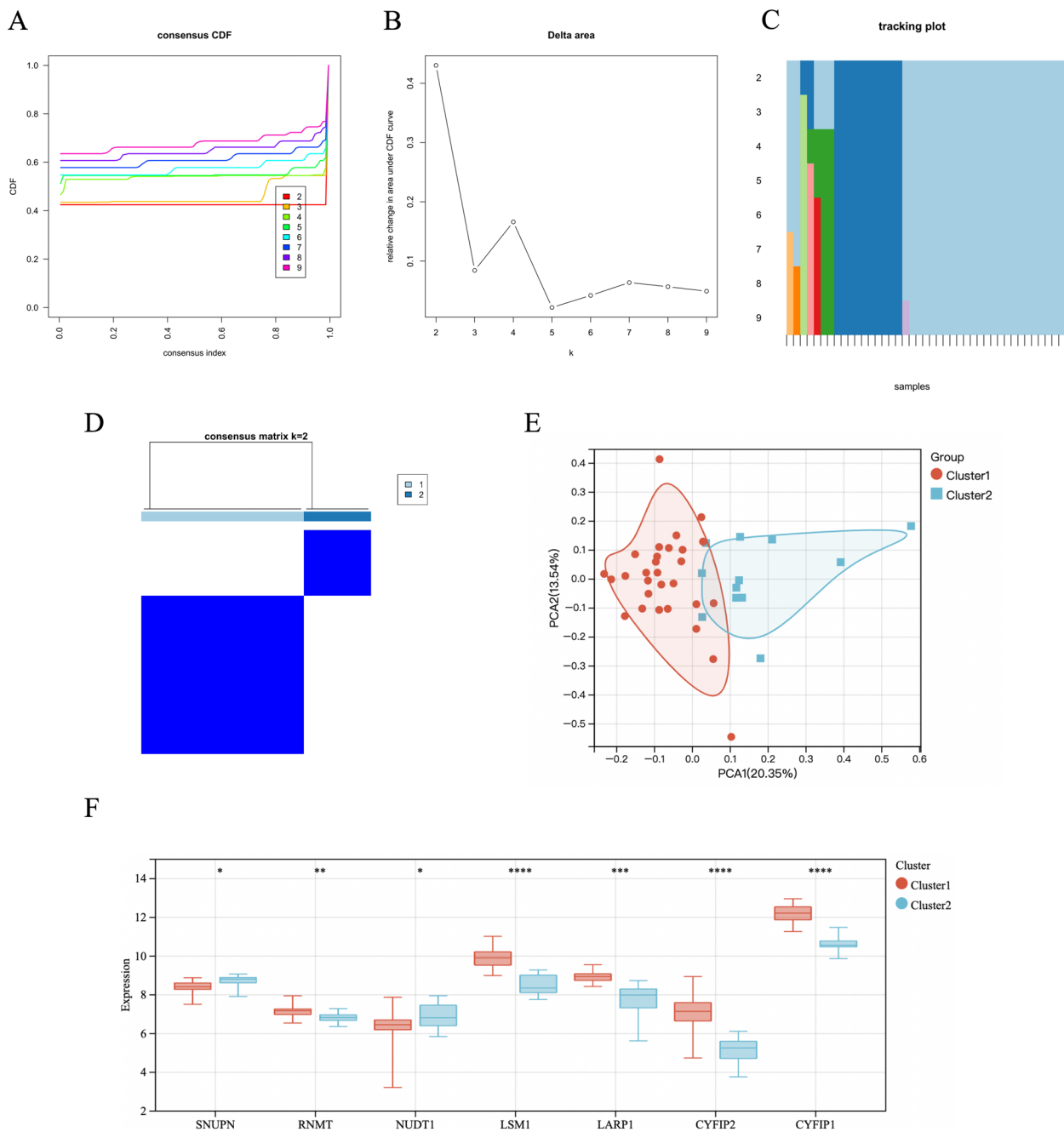


Fig. 8 Consensus clustering of the seven m7G hub genes in OA. **A** Cumulative distribution function (CDF) of consistent clustering for k=2–9. **B** Area fraction under the CDF curve for k=2–9. **C** The trace plot for k=2–9. **D** Heat map of scale matrix in the OA sample. **E** Principal component analysis (PCA): red for Cluster1 (C1), blue for Cluster 2 (C2), indicating the two m7G modification patterns were significantly different. **F** Box plot of consensus clustering of seven characteristic m7G RNA methylation regulators in the two m7G modification patterns

GSEA on C1 and C2. The findings of the study indicated a considerable enrichment of C1 in many biological processes, including nitrogen metabolism, GnRH signaling pathway, and long term potentiation, as observed in the KEGG database. The enrichment analysis revealed a high enrichment of C2 in parkinsons disease and ribosome,

as depicted in Fig. 9E. In the Reactome database, C1 was significantly enriched in DNA damage telomere stress induced senescence and regulation of mecp2 expression and activity. C2 was significantly enriched in translation, regulation of expression of slits and robos and influenza infection (Fig. 9F).

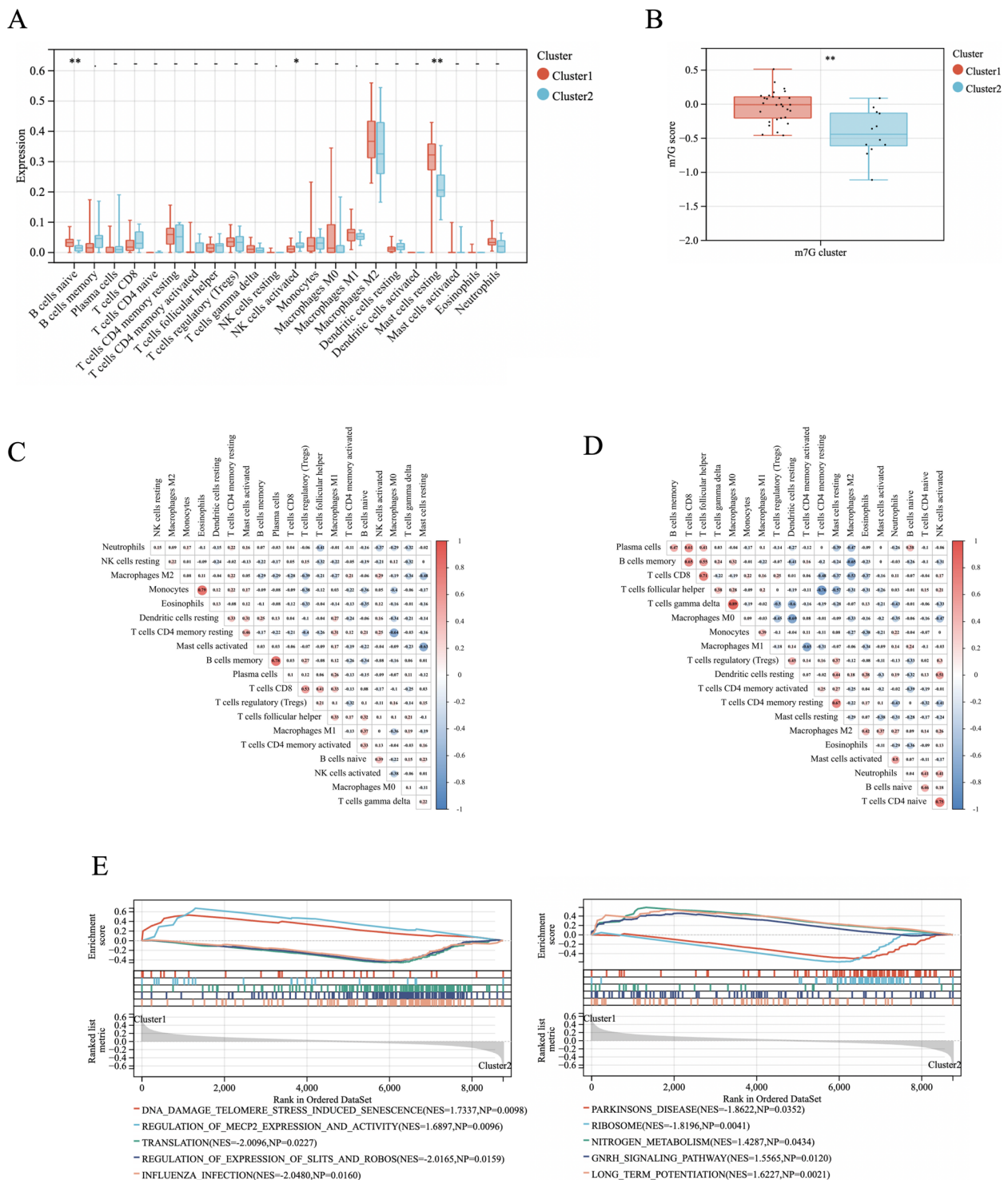


Fig. 9 Identification of the immune characteristics of m7G methylation patterns. **A** Box plot of differential expression of 22 immune cells in two m7G modification patterns. **B** The m7G score in two m7G patterns. **C, D** Correlations between 22 immune cells that significantly differed between C1 and C2 patients: correlations in C1 (**C**); correlations in C2 (**D**). **E** GSEA enrichment analysis

Validation of m7G hub genes

For our results, we used RT-qPCR to verify these 7 characteristic regulators associated with m7G RNA methylation. In OA synovial tissue, the expression of RNMT and LARP1 was significantly reduced in comparison to the control group. Conversely, CYFIP2, LSM1, SNUPN, NUDT1, and CYFIP1 exhibited considerably high expression levels (Fig. 10). These results were consistent with our predictions using bioinformatics tools.

Discussion

Osteoarthritis (OA) is a multifactorial disease influenced by metabolism, mechanical overload, trauma, inflammation, and genetic predisposition, with synovial inflammation playing a crucial role in disease progression [38, 39]. m7G modification, an essential epigenetic regulator of RNA function, has been implicated in various diseases, yet its role in OA and immune cell infiltration remains unclear. To investigate this, we performed bioinformatics analyses on microarray and high-throughput data, identifying m7G-related DEGs in OA and control samples. Using LASSO Cox regression, we pinpointed m7G hub genes strongly associated with OA and developed a predictive model. A ceRNA network was also constructed to explore post-transcriptional regulation and potential therapeutic targets. Further analysis of immune infiltration patterns led to the development of a scoring system to quantify m7G modification patterns, and RT-qPCR validation provided insights into the role of m7G in OA.

Gene microarray technology combined with bioinformatics analysis has proven effective in identifying key genes associated with various diseases, facilitating disease prediction and discovery of diagnostic and therapeutic targets. In this study, six datasets were integrated

as a training cohort, including 41 OA and 39 normal samples, with the model validated using two independent external cohorts. A total of 9 DEGs were identified among 22 m7G RNA methylation regulators, with SNUPN, NUDT1, LSM1, EIF4E2, CYFIP2, and CYFIP1 upregulated in OA, suggesting their role in OA progression. After univariate logistic analysis and LASSO Cox regression, we screened seven m7G hub genes and constructed a diagnostic model, achieving AUC values exceeding 0.8 across the training and validation cohorts, confirming its high diagnostic accuracy.

A nomogram was developed based on these seven m7G hub genes to predict OA risk. Genes were assigned scores, with a total score <150 corresponding to a <5% OA probability, while a score >230 indicated a >99% probability. The calibration curve confirmed the model's clinical utility, and RT-qPCR validation further supported our findings.

The combination of SNUPN, RNMT, NUDT1, LSM1, LARP1, CYFIP2, and CYFIP1 may serve as a novel biomarker for OA, playing a role in disease development and progression. Among them, SNUPN has also been linked to chronic lymphocytic leukemia and various cancers. The XPO1 protein, which binds to leucine-rich nuclear export signals at the N-terminus of SNUPN, has been found to be overexpressed or dysfunctional in multiple cancers [40, 41]. Chen et al. reported that SNUPN is upregulated in OA, suggesting its involvement in OA pathogenesis [23]. Similarly, Hao et al. constructed an m7G-related scoring model incorporating SNUPN to aid in OA diagnosis [40]. Our study further supports SNUPN as a potential biomarker, highlighting its prognostic significance in OA. While previous research has primarily focused on SNUPN's role in cancer, further

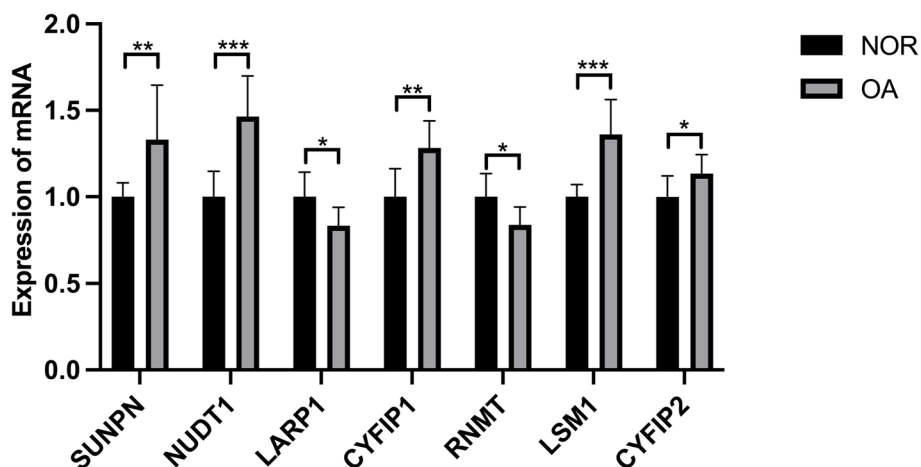


Fig. 10 Validation of m7G hub genes using RT-qPCR. The relative mRNA expressions of SNUPN, RNMT, NUDT1, LSM1, LARP1, CYFIP2, and CYFIP1 were displayed

comprehensive studies are needed to clarify its mechanistic involvement in OA.

LARP1 is located in cytoplasmic stress granules and colocalizes with the TORC1 complex and polysomal ribosome. LARP1 involved in several processes, including TORC1 signaling, cellular response to rapamycin, and posttranscriptional regulation of gene expression. GO annotations related to this gene include RNA binding and translation initiation factor binding. Hao et al. also identified LARP1 as a significant biomarker for distinguishing patients with OA from those without the condition [40], a finding that aligns with the results of our investigation.

RNMT is involved in 7-methylguanosine mRNA capping and facilitates RNA export and translation [42]. Among its related pathways are formation of HIV elongation complex in the absence of HIV tat and HIV life cycle. GO related to this gene include RNA binding and mRNA (guanine-N7-)-methyltransferase activity. Yin et al. first reported RNMT as a potential biomarker for OA and performed preliminary validation in OA cell models and clinical samples [43]. In addition, RNMT regulates the expression of the LARP1 target (TOP mRNA in the terminal polypyrimidine tract) in a selective manner. During T cell activation, an increase in ribosome abundance causes the upregulation of RNMT, which is responsible for coordinating mRNA capping and processing and enhancing translational capacity.

CYFIP1 encodes a protein that regulates cytoskeletal dynamics and protein translation. Reduced expression of this gene has been observed in various human cancers and the encoded protein may inhibit tumor invasion. Chen et al. identified CYFIP1 as a significant regulator of RNA modification in OA, which examined the biomarkers and m7G modification pattern in the immune microenvironment of OA [23]. Our study also proved this.

CYFIP2 has been shown to play an important regulatory role in the central nervous system [44]. CYFIP2 showed a significant relationship with immunomodulatory factors and immune-related genes. It can be used as a cancer biomarker to determine the prognosis and may be a promising treatment strategy for tumor immunotherapy [45]. The protein encoded by NUDT1 is an enzyme that hydrolyzes oxidized purine nucleoside triphosphates, which inhibits carcinogenesis and neurodegenerative diseases. NUDT1 may play an important role in the development of gliomas and clear cell renal cell carcinoma through activation of HIF-1 α expression [46, 47]. LSM1 is known to participate in the general process of mRNA degradation in complexes that contain LSm subunits [48]. Overexpression of LSM1 has been shown to promote the tumor transformation, proliferation, chemoresistance, and metastasis [49]. Our study is the first one to show that CYFIP2, NUDT1 and LSM1

may have an impact on the pathogenesis of OA, but it still needs further exploration.

We conducted functional enrichment analysis of hub regulators using GO and KEGG, revealing their involvement in mRNA metabolic processes, mRNA cap binding, RNA binding, and RNA transport, suggesting a strong connection to mRNA regulation. m7G modification, a highly conserved RNA modification, is present in the 5' cap structure of tRNAs, rRNAs, and mRNAs, playing a critical role in RNA processing, metabolism, and function [23, 40]. Our findings highlight the impact of m7G modification on mRNA cap synthesis, particularly in OA-associated mRNAs, where it influences translation, splicing, stability, and protein synthesis.

miRNAs, small non-coding RNAs (~22 nt), regulate gene expression post-transcriptionally and are implicated in tissue damage and disease progression [50]. As potential therapeutic targets, miRNAs have been linked to OA [51], heart failure [52], and diabetes [53]. Our miRNA-target gene network analysis identified hsa-mir-1-3p and hsa-mir-16-5p as key regulators. Hsa-mir-1-3p has been associated with type 1 diabetes and perioperative myocardial injury [54, 55], while hsa-mir-16-5p plays a role in neuroblastoma and osteosarcoma [56]. Further studies are needed to validate their potential as OA biomarkers, but these findings pave the way for precision diagnostics and targeted therapy in OA. Additionally, drug target prediction suggested that chlortetracycline HL60 DOWN, PARAQUAT CTD 00006471, and baclofen HL60 DOWN may have therapeutic potential for OA. However, further experimental validation is required to confirm their clinical efficacy in OA treatment.

Numerous studies have highlighted the crucial role of the immune response in OA pathogenesis, with m7G methylation regulators implicated in immune infiltration [57–59]. OA is characterized by inflammatory infiltration of macrophages, T cells, mast cells, B cells, plasma cells, NK cells, dendritic cells, and granulocytes within the synovium [15]. The innate immune system is activated in response to cellular stress and extracellular matrix degradation, underscoring the importance of modulating immune responses as a therapeutic approach for OA [60].

In this study, we found that OA patients exhibited increased infiltration of activated CD4+ memory T cells, Tregs, M0/M1 macrophages, and resting mast cells, while resting CD4+ memory T cells, activated mast cells, and eosinophils were significantly reduced. Macrophages, the predominant immune cells in the synovium, play a central role in immune recruitment, inflammatory injury, and extracellular matrix degradation [61]. Notably, M1 macrophages, which infiltrate the OA synovium, contribute to pain, joint space narrowing, and osteophyte

formation through the secretion of inflammatory mediators [13, 62]. T cells, particularly CD4+ memory T cells, are also critical in OA pathology. Studies have shown that CD4+ T cells accumulate in the synovial lining of OA patients, contributing to chronic inflammation [63, 64]. Additionally, Tregs, known for their immunomodulatory function, regulate inflammatory cytokine production in OA, with their levels closely correlating with inflammatory factors [65–67]. Mast cells have also been implicated in OA progression, with studies demonstrating a positive correlation between mast cell abundance, synovitis severity, and radiographic disease progression [68, 69]. Experimental models lacking mast cells exhibit reduced arthritis severity, further supporting their role in OA pathophysiology [70]. However, the role of eosinophils in OA remains unclear and warrants further investigation.

To better understand the functional implications of m7G methylation in OA, we performed molecular subtyping using Consensus Clustering. Our analysis identified two distinct m7G modification patterns (C1 and C2), each displaying unique gene expression profiles and immune infiltration characteristics. C1 was associated with higher levels of naive B cells and resting mast cells, while C2 exhibited greater NK cell abundance. Given that B lymphocytic infiltration correlates with OA severity, and B cells secrete pro-inflammatory mediators that promote cartilage destruction [71–73], the immune differences between the two clusters may reflect distinct OA pathophysiological mechanisms. NK cells, particularly CD16+CD56+ subsets, have been implicated in OA, potentially influencing disease progression through adhesion mechanisms [74]. Our findings suggest that m7G methylation plays a key role in OA synovitis, shaping the immune microenvironment and contributing to disease heterogeneity. However, further experimental validation is needed to elucidate the precise mechanisms. To quantify these m7G modification patterns, we developed an m7G scoring system using PCA. Consistent with previous studies [23], we found that C1 was associated with inflammatory phenotypes, while C2 correlated with non-inflammatory OA phenotypes. This classification strategy enhances our understanding of immune regulation in OA and may aid in the development of individualized therapeutic strategies.

Compared to previous studies [23, 75, 76], our research provides several key innovations. While previous works have explored hub genes and immune infiltration in OA, they have not systematically investigated the role of m7G modification in regulating the OA immune microenvironment. Our study is the first to reveal the association between m7G genes and immune cell infiltration, such as CYFIP2 had the strongest positive correlation with memory B cells ($r=0.50$),

highlighting its impact on immune dysregulation. Additionally, while prior studies have focused on drug target prediction, they did not establish a robust diagnostic model; we applied LASSO-Cox regression to identify seven key m7G hub genes and developed a Nomogram-based risk prediction model with AUCs of 0.96 (training set), 0.93/0.84 (validation cohorts), significantly improving OA risk assessment. Furthermore, unlike previous studies that relied solely on bioinformatics, we conducted RT-qPCR validation of seven hub genes in clinical OA samples, providing strong experimental support for potential clinical applications. Overall, our study integrates m7G modification, immune infiltration, diagnostic modeling, and experimental validation, offering new mechanistic insights and translational potential in OA research.

Conclusion

This study is the first to highlight the pivotal role of SNUPN, RNMT, NUDT1, LSM1, LARP1, CYFIP2, and CYFIP1 in OA, offering fresh insights into OA pathogenesis and identifying promising biomarkers. Using these seven hub genes, we developed a risk prediction model with strong accuracy for OA diagnosis. Additionally, two distinct m7G modification patterns related to immune cell infiltration were identified, with gene expression levels validated through RT-qPCR. These findings provide new perspectives on the immune regulation mechanisms of OA, opening avenues for improved diagnosis and treatment strategies. Further research is needed to deepen understanding of these mechanisms.

Abbreviations

OA	Osteoarthritis
IPFP	Infrapatellar Fat Pad
LASSO	Least Absolute Shrinkage and Selection Operator
GEO	Gene Expression Omnibus
PCA	Principal Component Analysis
DEGs	Differentially Expressed Genes
GSEA	Gene Set Enrichment Analysis
RT-qPCR	Real-Time quantitative Polymerase Chain Reaction
PPI	Protein–Protein Interaction
AUC	Area Under the Curve
ROC	Receiver Operating Characteristic
UMAP	Uniform Manifold Approximation and Projection
NK	Natural Killer

Supplementary Information

The online version contains supplementary material available at <https://doi.org/10.1186/s12891-025-08539-6>.

Additional file 1: Table S1. 40 m7G-related genes and 22 of the 40 m7G-related genes are present in the synovium. Table S2. The primer sequences for the genes. Table S3. Basic information of the datasets included in this study.

Acknowledgements

We thank all the participants for participating in our study.

Authors' contributions

ZH, YN, and FW contributed to the conception and design of the research. Material preparation, data collection, and analysis were performed by CF. The first draft of the manuscript was written by ZH. KL and CX prepared all the figures and the tables. All authors commented on previous versions of the manuscript. And all authors read and approved the final manuscript.

Funding

The author(s) received no financial support for the research, authorship, and/or publication of this article.

Data availability

All data used to support the findings of this study are included within the article. The datasets used and analyzed during the current study are available from GEO (<http://www.ncbi.nlm.nih.gov/geo>). The analyzed datasets generated during the study are available from the corresponding author upon reasonable request.

Declarations

Ethics approval and consent to participate

The studies involving human participants were reviewed and approved by the Ethics Committee of the Third Hospital of Hebei Medical University (Ke2024-106-1). The patients/participants provided their written informed consent to participate in this study.

Consent for publication

Written informed consent was obtained from all individuals.

Competing interests

The authors declare no competing interests.

Received: 9 February 2024 Accepted: 17 March 2025

Published online: 04 April 2025

References

- Bijlsma JW, Berenbaum F, Lefeber FP. Osteoarthritis: an update with relevance for clinical practice. *Lancet*. 2011;377(9783):2115–26.
- Berenbaum F. Osteoarthritis as an inflammatory disease (osteoarthritis is not osteoarthrosis!). *Osteoarthritis Cartilage*. 2013;21(1):16–21.
- Dobson GP, Letson HL, Grant A, McEwen P, Hazratwala K, Wilkinson M, Morris JL. Defining the osteoarthritis patient: back to the future. *Osteoarthritis Cartilage*. 2018;26(8):1003–7.
- Prieto-Potin I, Largo R, Roman-Blas JA, Herrero-Baumont G, Walsh DA. Characterization of multinucleated giant cells in synovium and subchondral bone in knee osteoarthritis and rheumatoid arthritis. *BMC Musculoskelet Disord*. 2015;16:226.
- Palazzo C, Nguyen C, Lefevre-Colau MM, Rannou F, Poiraudou S. Risk factors and burden of osteoarthritis. *Ann Phys Rehabil Med*. 2016;59(3):134–8.
- Hao Z, Wang Y, Wang L, Feng Q, Li H, Chen T, et al. Burden evaluation and prediction of osteoarthritis and site-specific osteoarthritis coupled with attributable risk factors in China from 1990 to 2030. *Clin Rheumatol*. 2024;43(6):2061–77.
- Rahmati M, Nalesso G, Mobasheri A, Mozafari M. Aging and osteoarthritis: central role of the extracellular matrix. *Ageing Res Rev*. 2017;40:20–30.
- Kulkarni K, Karssiens T, Kumar V, Pandit H. Obesity and osteoarthritis. *Maturitas*. 2016;89:22–8.
- Zhai G, Huang J. Genetics of osteoarthritis. *Best Pract Res Clin Rheumatol*. 2024;38(4): 101972.
- Li Z, Zhang S, Mao G, Xu Y, Kang Y, Zheng L, et al. Identification of anterior cruciate ligament fibroblasts and their contribution to knee osteoarthritis progression using single-cell analyses. *Int Immunopharmacol*. 2023;125(Pt A): 111109.
- Sampath SJP, Venkatesan V, Ghosh S, Kotikalapudi N. Obesity, metabolic syndrome, and osteoarthritis—an updated review. *Curr Obes Rep*. 2023;12(3):308–31.
- Vincent TL. Targeting mechanotransduction pathways in osteoarthritis: a focus on the pericellular matrix. *Curr Opin Pharmacol*. 2013;13(3):449–54.
- Sanchez-Lopez E, Coras R, Torres A, Lane NE, Guma M. Synovial inflammation in osteoarthritis progression. *Nat Rev Rheumatol*. 2022;18(5):258–75.
- Xiao P, Han X, Huang Y, Yang J, Chen L, Cai Z, et al. Reprogramming macrophages via immune cell mobilized hydrogel microspheres for osteoarthritis treatments. *Bioact Mater*. 2024;32:242–59.
- Li YS, Luo W, Zhu SA, Lei GH. T cells in osteoarthritis: alterations and beyond. *Front Immunol*. 2017;8:356.
- Sui X, Hu Y, Ren C, Cao Q, Zhou S, Cao Y, et al. METTL3-mediated m(6A) is required for murine oocyte maturation and maternal-to-zygotic transition. *Cell Cycle*. 2020;19(4):391–404.
- Liu L, Wang J, Sun G, Wu Q, Ma J, Zhang X, et al. m(6A) mRNA methylation regulates CTNNB1 to promote the proliferation of hepatoblastoma. *Mol Cancer*. 2019;18(1):188.
- Gao Y, Vasic R, Song Y, Teng R, Liu C, Gblyl R, et al. m(6A) modification prevents formation of endogenous double-stranded RNAs and deleterious innate immune responses during hematopoietic development. *Immunity*. 2020;52(6):1007–1021.e1008.
- Zhang H, Shi X, Huang T, Zhao X, Chen W, Gu N, Zhang R. Dynamic landscape and evolution of m6A methylation in human. *Nucleic Acids Res*. 2020;48(11):6251–64.
- Luo Y, Yao Y, Wu P, Zi X, Sun N, He J. The potential role of N(7)-methylguanosine (m7G) in cancer. *J Hematol Oncol*. 2022;15(1):63.
- Malbec L, Zhang T, Chen YS, Zhang Y, Sun BF, Shi BY, et al. Dynamic methylome of internal mRNA N(7)-methylguanosine and its regulatory role in translation. *Cell Res*. 2019;29(11):927–41.
- Backlund M, Stein F, Rettel M, Schwarzl T, Perez-Perri JI, Brosig A, et al. Plasticity of nuclear and cytoplasmic stress responses of RNA-binding proteins. *Nucleic Acids Res*. 2020;48(9):4725–40.
- Chen Z, Hua Y. Identification of m7G-related hub biomarkers and m7G regulator expression pattern in immune landscape during the progression of osteoarthritis. *Cytokine*. 2023;170: 156313.
- Katsara O, Schneider RJ. m(7)G tRNA modification reveals new secrets in the translational regulation of cancer development. *Mol Cell*. 2021;81(16):3243–5.
- Johnson WE, Li C, Rabinovic A. Adjusting batch effects in microarray expression data using empirical Bayes methods. *Biostatistics*. 2007;8(1):118–27.
- Szklarczyk D, Gable AL, Lyon D, Junge A, Wyder S, Huerta-Cepas J, et al. STRING v11: protein-protein association networks with increased coverage, supporting functional discovery in genome-wide experimental datasets. *Nucleic Acids Res*. 2019;47(D1):D607–d613.
- Shannon P, Markiel A, Ozier O, Baliga NS, Wang JT, Ramage D, et al. Cytoscape: a software environment for integrated models of biomolecular interaction networks. *Genome Res*. 2003;13(11):2498–504.
- An J, Lai J, Sajjanhar A, Batra J, Wang C, Nelson CC. J-Circos: an interactive Circos plotter. *Bioinformatics*. 2015;31(9):1463–5.
- Wang L, Wei S, Zhou B, Wu S. A nomogram model to predict the venous thromboembolism risk after surgery in patients with gynecological tumors. *Thromb Res*. 2021;202:52–8.
- Wilkerson MD, Hayes DN. ConsensusClusterPlus: a class discovery tool with confidence assessments and item tracking. *Bioinformatics*. 2010;26(12):1572–3.
- Kanehisa M, Goto S. KEGG: kyoto encyclopedia of genes and genomes. *Nucleic Acids Res*. 2000;28(1):27–30.
- Shen W, Song Z, Zhong X, Huang M, Shen D, Gao P, et al. Sangerbox: a comprehensive, interaction-friendly clinical bioinformatics analysis platform. *iMeta*. 2022;1(3):e36.
- Fan Y, Siklenka K, Arora SK, Ribeiro P, Kimmins S, Xia J. miRNet - dissecting miRNA-target interactions and functional associations through network-based visual analysis. *Nucleic Acids Res*. 2016;44(W1):W135–141.
- Newman AM, Steen CB, Liu CL, Gentles AJ, Chaudhuri AA, Scherer F, et al. Determining cell type abundance and expression from bulk tissues with digital cytometry. *Nat Biotechnol*. 2019;37(7):773–82.
- Zhang Y, Liu N, Wang S. A differential privacy protecting K-means clustering algorithm based on contour coefficients. *PLoS ONE*. 2018;13(11): e0206832.

36. Subramanian A, Tamayo P, Mootha VK, Mukherjee S, Ebert BL, Gillette MA, et al. Gene set enrichment analysis: a knowledge-based approach for interpreting genome-wide expression profiles. *Proc Natl Acad Sci U S A*. 2005;102(43):15545–50.
37. Liberzon A, Subramanian A, Pinchback R, Thorvaldsdóttir H, Tamayo P, Mesirov JP. Molecular signatures database (MSigDB) 3.0. *Bioinformatics*. 2011;27(12):1739–40.
38. Allen KD, Thoma LM, Golightly YM. Epidemiology of osteoarthritis. *Osteoarthritis Cartilage*. 2022;30(2):184–95.
39. Nedunchezhiyan U, Varughese I, Sun AR, Wu X, Crawford R, Prasadam I. Obesity, inflammation, and immune system in osteoarthritis. *Front Immunol*. 2022;13: 907750.
40. Hao L, Shang X, Wu Y, Chen J, Chen S. Construction of a diagnostic m(7)G regulator-mediated scoring model for identifying the characteristics and immune landscapes of osteoarthritis. *Biomolecules*. 2023;13(3):539–53.
41. Jain P, Kanagal-Shamanna R, Wierda W, Keating M, Sarwari N, Rozovsky U, et al. Clinical and molecular characteristics of XPO1 mutations in patients with chronic lymphocytic leukemia. *Am J Hematol*. 2016;91(11):E478–e479.
42. Bueren-Calabuig JA, G. Bage M, Cowling VH, Pislakov AV. Mechanism of allosteric activation of human mRNa cap methyltransferase (RNMT) by RAM: insights from accelerated molecular dynamics simulations. *Nucleic Acids Res*. 2019;47(16):8675–92.
43. Yin W, Lei Y, Yang X, Zou J. A two-gene random forest model to diagnose osteoarthritis based on RNA-binding protein-related genes in knee cartilage tissue. *Aging (Albany NY)*. 2023;15(1):193–212.
44. Schaks M, Reinke M, Witke W, Rottner K. Molecular dissection of neurodevelopmental disorder-causing mutations in CYFIP2. *Cells*. 2020;9(6):1355.
45. Peng Q, Ren B, Xin K, Liu W, Alam MS, Yang Y, et al. CYFIP2 serves as a prognostic biomarker and correlates with tumor immune microenvironment in human cancers. *Eur J Med Res*. 2023;28(1):364.
46. Wu Y, Liu L, Huang D, Li Z, Xu R, Cheng M, et al. Uncover DNA damage and repair-related gene signature and risk score model for glioma. *Ann Med*. 2023;55(1): 2200033.
47. Shi J, Xiong Z, Wang K, Yuan C, Huang Y, Xiao W, et al. HIF2 α promotes tumour growth in clear cell renal cell carcinoma by increasing the expression of NUDT1 to reduce oxidative stress. *Clin Transl Med*. 2021;11(11): e592.
48. Tzeng YT, Tsui KH, Tseng LM, Hou MF, Chu PY, Sheu JJ, Li CJ. Integrated analysis of pivotal biomarker of LSM1, immune cell infiltration and therapeutic drugs in breast cancer. *J Cell Mol Med*. 2022;26(14):4007–20.
49. Little EC, Camp ER, Wang C, Watson PM, Watson DK, Cole DJ. The CaSm (LSM1) oncogene promotes transformation, chemoresistance and metastasis of pancreatic cancer cells. *Oncogenesis*. 2016;5(1): e182.
50. Makarova J, Turchinovich A, Shkurnikov M, Tonevitsky A. Extracellular miRNAs and cell-cell communication: problems and prospects. *Trends Biochem Sci*. 2021;46(8):640–51.
51. Li J, Gao X, Zhu W, Li X. Integrative analysis of the expression of microRNA, Long Noncoding RNA, and mRNA in Osteoarthritis and Construction of a Competing Endogenous Network. *Biochem Genet*. 2022;60(4):1141–58.
52. Fang X, Song R, Wei J, Liao Q, Zeng Z. Mining potential drug targets and constructing diagnostic models for heart failure based on miRNA-mRNA networks. *Mediators Inflamm*. 2022;2022:9652169.
53. Yan YX, Dong J, Li YL, Lu YK, Yang K, Wang T, et al. CircRNA hsa_circ_0071336 is associated with type 2 diabetes through targeting the miR-93-5p/GLUT4 axis. *Faseb j*. 2022;36(5): e22324.
54. May SM, Abbott TEF, Del Arroyo AG, Reyes A, Martir G, Stephens RCM, et al. MicroRNA signatures of perioperative myocardial injury after elective noncardiac surgery: a prospective observational mechanistic cohort study. *Br J Anaesth*. 2020;125(5):661–71.
55. Morales-Sánchez P, Lambert C, Ares-Blanco J, Suárez-Gutiérrez L, Villa-Fernández E, García AV, et al. Circulating miRNA expression in long-standing type 1 diabetes mellitus. *Sci Rep*. 2023;13(1):8611.
56. Ghafouri-Fard S, Khoshbakht T, Hussen BM, Abdullah ST, Taheri M, Samadian M. A review on the role of mir-16-5p in the carcinogenesis. *Cancer Cell Int*. 2022;22(1):342.
57. Huang T, He WY. Construction and validation of a novel prognostic signature of idiopathic pulmonary fibrosis by identifying subtypes based on genes related to 7-Methylguanosine modification. *Front Genet*. 2022;13: 890530.
58. Li XY, Zhao ZJ, Wang JB, Shao YH, Hui L, You JX, Yang XT. m7G methylation-related genes as biomarkers for predicting overall survival outcomes for hepatocellular carcinoma. *Front Bioeng Biotechnol*. 2022;10: 849756.
59. Zeng X, Liao G, Li S, Liu H, Zhao X, Li S, et al. Eliminating METTL1-mediated accumulation of PMN-MDSCs prevents hepatocellular carcinoma recurrence after radiofrequency ablation. *Hepatology*. 2023;77(4):1122–38.
60. Kraus VB, Blanco FJ, Englund M, Karsdal MA, Lohmander LS. Call for standardized definitions of osteoarthritis and risk stratification for clinical trials and clinical use. *Osteoarthritis Cartilage*. 2015;23(8):1233–41.
61. Fernandes TL, Gomoll AH, Lattermann C, Hernandez AJ, Bueno DF, Amanó MT. Macrophage: a potential target on cartilage regeneration. *Front Immunol*. 2020;11: 111.
62. Zhang L, Chen X, Cai P, Sun H, Shen S, Guo B, Jiang Q. Reprogramming mitochondrial metabolism in synovial macrophages of early osteoarthritis by a camouflaged meta-defensome. *Adv Mater*. 2022;34(30): e2202715.
63. Haynes MK, Hume EL, Smith JB. Phenotypic characterization of inflammatory cells from osteoarthritic synovium and synovial fluids. *Clin Immunol*. 2002;105(3):315–25.
64. Ezawa K, Yamamura M, Matsui H, Ota Z, Makino H. Comparative analysis of CD45RA- and CD45RO-positive CD4+T cells in peripheral blood, synovial fluid, and synovial tissue in patients with rheumatoid arthritis and osteoarthritis. *Acta Med Okayama*. 1997;51(1):25–31.
65. Xia J, Ni Z, Wang J, Zhu S, Ye H. Overexpression of lymphocyte activation gene-3 inhibits regulatory T cell responses in osteoarthritis. *DNA Cell Biol*. 2017;36(10):862–9.
66. Raphael I, Nalawade S, Eagar TN, Forsthuber TG. T cell subsets and their signature cytokines in autoimmune and inflammatory diseases. *Cytokine*. 2015;74(1):5–17.
67. Miyara M, Sakaguchi S. Natural regulatory T cells: mechanisms of suppression. *Trends Mol Med*. 2007;13(3):108–16.
68. de Lange-Brokaar BJ, Kloppenburg M, Andersen SN, Dorjée AL, Yusuf E, Herb-van Toorn L, et al. Characterization of synovial mast cells in knee osteoarthritis: association with clinical parameters. *Osteoarthritis Cartilage*. 2016;24(4):664–71.
69. Pu J, Nishida K, Inoue H, Asahara H, Ohtsuka A, Murakami T. Mast cells in osteoarthritic and rheumatoid arthritic synovial tissues of the human knee. *Acta Med Okayama*. 1998;52(1):35–9.
70. Lee DM, Friend DS, Gurish MF, Benoist C, Mathis D, Brenner MB. Mast cells: a cellular link between autoantibodies and inflammatory arthritis. *Science*. 2002;297(5587):1689–92.
71. Da RR, Qin Y, Baeten D, Zhang Y. B cell clonal expansion and somatic hypermutation of Ig variable heavy chain genes in the synovial membrane of patients with osteoarthritis. *J Immunol*. 2007;178(1):557–65.
72. Wu F, Gao J, Kang J, Wang X, Niu Q, Liu J, Zhang L. B cells in rheumatoid arthritis: pathogenic mechanisms and treatment prospects. *Front Immunol*. 2021;12: 750753.
73. Fang Q, Zhou C, Nandakumar KS. Molecular and cellular pathways contributing to joint damage in rheumatoid arthritis. *Mediators Inflamm*. 2020;2020:3830212.
74. Lin J, Xiao L, Ouyang G, Shen Y, Huo R, Zhou Z, et al. Total glucosides of paeony inhibits Th1/Th17 cells via decreasing dendritic cells activation in rheumatoid arthritis. *Cell Immunol*. 2012;280(2):156–63.
75. Wu ZY, Du G, Lin YC. Identifying hub genes and immune infiltration of osteoarthritis using comprehensive bioinformatics analysis. *J Orthop Surg Res*. 2021;16(1):630.
76. Xu W, Wang X, Liu D, Lin X, Wang B, Xi C, et al. Identification and validation of hub genes and potential drugs involved in osteoarthritis through bioinformatics analysis. *Front Genet*. 2023;14: 1117713.

Publisher's Note

Springer Nature remains neutral with regard to jurisdictional claims in published maps and institutional affiliations.